



# Computed tomographic evaluation of glenoid joint line restoration with glenoid bone grafting and reverse shoulder arthroplasty in patients with significant glenoid bone loss

Kristine R. Italia, MD, FPOA<sup>a,b,\*</sup>, Nicholas Green, BDes, MEng<sup>b</sup>,  
Jashint Maharaj, MBBS, MPHTM<sup>b,c</sup>, Marine Launay, MEng<sup>b,c</sup>,  
Ashish Gupta, MBBS, MSc, FRACS, FAOrthA<sup>a,b,c</sup>

<sup>a</sup>Greenslopes Private Hospital, Brisbane, Australia

<sup>b</sup>Queensland Unit for Advanced Shoulder Research (QUASR), Brisbane, Australia

<sup>c</sup>Shoulder Surgery QLD Research Institute, Brisbane, Australia

**Background:** Restoration of native glenohumeral joint line is important for a successful outcome after reverse shoulder arthroplasty (RSA). The aims of this study were to quantify the restoration of glenoid joint line after structural bone grafting and RSA, and to evaluate graft incorporation, correction of glenoid version, and rate of notching.

**Methods:** This is a retrospective review of 21 patients who underwent RSA (20 primary, 1 revision) with glenoid bone grafting (15 autografts, 6 allografts). Grammont design implants and baseplate with long peg were used in all patients. Preoperative and postoperative 3D models were created using MIMICS 21.0. Preoperative defects were classified, and postoperative joint line restoration was assessed based on the lateral aspect of the base of the coracoid. Postoperative computed tomographic (CT) scans were evaluated for graft incorporation, version correction, and presence of notching.

**Results:** Preoperative glenoid defects were classified as massive (5%), large (29%), moderate (52%), and small (14%). The average preoperative version was 8° of retroversion. The average postoperative version was 5° of retroversion. The average preoperative medialization was noted to be 8.4 mm medial to native joint line or 0.6 mm (range –16.8 to 13.2) lateral to the coracoid base. The postoperative CT scans demonstrated a mean joint line at 12.1 mm (range 1.3–22.4) lateral to the coracoid base. At the 3-month follow-up, all patients demonstrated graft incorporation on CT scans. Graft osteolysis was observed on CT scan in 4.8% of patients at a mean follow-up of 19.5 months.

**Discussion:** Structural bone grafting of glenoid defect effectively re-creates the glenoid anatomy, restores glenoid bone stock, re-creates the true glenohumeral joint line, and corrects glenoid deformity. The use of bone grafting also allows lateralization of the baseplate and glenosphere, reducing the risk of severe scapular notching.

**Conclusion:** Restoration of the glenoid joint line was achieved in all patients. Glenoid bone grafting is a viable option for restoring glenoid joint line in cases of significant glenoid defects encountered during RSA.

Institutional Review Board approval was received from the Greenslopes Research and Ethics Committee (protocol 19/08).

\*Reprint requests: Kristine R. Italia, MD, FPOA, Greenslopes Hospital, Suite 306, Level 9, Nicholson Street Specialist Center, 121 Newdegate St., Brisbane, Australia.

E-mail address: [kristine\\_italia@yahoo.com](mailto:kristine_italia@yahoo.com) (K.R. Italia).

**Level of Evidence:** Level IV; Case Series; Treatment Study

© 2020 Journal of Shoulder and Elbow Surgery Board of Trustees. All rights reserved.

**Keywords:** Glenoid defect; bone grafting; reverse shoulder arthroplasty; glenoid joint line

Reverse shoulder arthroplasty (RSA) has become a reliable surgical procedure to manage a spectrum of shoulder pathology including cuff tear arthropathy, osteoarthritis, irreparable cuff tear, and complex proximal humeral fractures. Glenoid bone loss of varying severity is routinely encountered when treating arthritis of the glenohumeral joint. Significant glenoid bone defects medialize the native glenoid joint line. Significant medialization of the joint line has undesirable effects on clinical outcomes after shoulder arthroplasty.<sup>18</sup> Excessive medialization can result in implant malpositioning. This can lead to post-operative impingement subsequently causing limited range of motion and scapular notching in the long term. Glenohumeral impingement can also produce prosthetic instability, aggravated by the presence of poor soft tissue tension because of the medialized construct.

Several techniques have been described to address glenoid bone loss. Eccentric reaming is one option to correct glenoid wear. Satisfactory outcomes are reported with preferentially reaming the glenoid.<sup>16,33</sup> However, it is recommended only for mild defects with retroversion of less than 15°. <sup>6,20</sup> Performing this in more severe cases of glenoid erosion may result in excessive removal of glenoid bone, compromising the quality of the available bone stock and medialization of the joint line.<sup>5,28</sup> The use of augmented glenoid baseplates and custom-made implants is a relatively new approach to address glenoid defects. Use of augmented baseplates aims to minimize bone removal on the glenoid. Good results are reported after use of these metallic augments.<sup>19,21</sup> However, these implants may not always be available, and at times the cost is prohibitive. Metallic complications such as development of metallic debris have been reported.<sup>8</sup> Furthermore, this technique does not restore glenoid bone stock, and future bone loss could pose a problem if revision surgery is required.

Bone grafting of the glenoid is another option for significant centric or eccentric glenoid defects. The aim is to biologically restore the glenoid anatomy and resultant correction of the glenoid joint line. Surgical techniques documented use of femoral head allografts to reconstruct massive uncontained glenoid defects.<sup>1</sup> Similarly, introduction of the bony increased-offset RSA (BIO-RSA) concept allowed for correction of glenoid deformity in terms of version and inclination using autograft harvested from the native humeral head and placed in between the reamed glenoid and the baseplate.<sup>3,4</sup> Satisfactory clinical outcomes are reported after bone grafting and RSA.<sup>4,15</sup> However, most of the studies reporting on the radiologic outcomes after bone grafting and RSA have focused on the correction

of glenoid version, evaluation of graft incorporation, assessing the presence or absence of scapular notching, graft resorption, and implant loosening. These were mostly evaluated on 2-dimensional (2D) images.<sup>3,4,22,25,26,32</sup> To our knowledge, literature on restoration of the native glenoid joint line achieved after bone grafting is limited.

Restoration of the glenoid anatomy and glenohumeral joint line is crucial for a successful outcome after RSA, and to avoid the undesirable effects due to glenoid bone loss and joint line medialization. The glenoid anatomy recreation is necessary to achieve correct implant placement, implant stability, and impingement-free range of motion. Lateralization of the joint line is an acceptable technique to attain deltoid wrap and improve the lever arm of the posterior deltoid and the posterior cuff. However, overlateralization may be associated with acromial stress fractures, traction neurologic injuries, coracoid tip pain, and inability to repair the rotator cuff and subscapularis.

Given these effects of joint line medialization and overlateralization, it is imperative for the glenoid joint line to be restored. The primary aim of our study is to quantify the restoration of glenoid joint line after structural bone grafting and RSA in patients with significant glenoid bone loss using standardized measurements on 3-dimensional (3D) reconstructed computed tomography (CT) images. The secondary aims are to evaluate the incorporation of bone graft into the native glenoid, the correction of glenoid version, and the rate of scapular notching. We hypothesize that glenoid bone grafting is an effective technique to accurately restore the glenoid joint line, correct version in patients with significant glenoid bone loss, has high rate of graft incorporation, and avoids scapular notching.

## Materials and methods

This was a retrospective review of prospectively collected data of consecutive patients who underwent RSA with glenoid bone grafting for significant glenoid bone loss in a single center performed by a single fellowship-trained orthopedic surgeon. Ethics approval was obtained from the institutional Human Ethics Review Committee.

Patients who underwent RSA with glenoid bone grafting from July 2016 to July 2018 were included in the study. Inclusion criteria were primary RSA and 2-stage revision RSA. Patients who had either humeral head autograft or femoral head allograft for the bone grafting were both included. Patients were excluded if they had incomplete follow-up data or less than 3-month radiologic (CT) follow-up. Patients who underwent 1-stage revision RSA were excluded due to study preference for prosthesis-free glenoid.

Intraoperative CT-based quantification of the amount of glenoid bone loss resulting from the removal of prosthesis during 1-stage revisions was not possible.

As part of standard clinical practice, all patients were preoperatively assessed using multislice CT of the whole scapula and whole humerus with standardized clinical settings (120-140 kVp,  $512 \times 512$  resolution, slice thickness 1.00 mm). Using the 2D images, their preoperative glenoid defects were classified according to the Gupta-Seebauer classification and treated according to the recommended guidelines.<sup>15</sup> Patients underwent single-stage RSA with bone grafting if they met the 50% rule criterion, whereby a minimum of 30%-50% of the baseplate or the baseplate-bone graft composite is resting on the native glenoid, 50% of the central peg is in the native scapula, and at least 2 opposite locking screws are in the native scapula.<sup>15</sup> Those who did not meet the criteria underwent a 2-stage bone grafting procedure.<sup>15</sup> Repeat CT scans were then performed postoperatively at 3 months, 1 year, and 5 years.

The images in Digital Imaging in Communications and Medicine (DICOM) format from the preoperative and most recent postoperative CT scans were reconstructed using medical imaging software (MIMICS 21.0; Materialise, Leuven, Belgium). As described in Green et al, the data were segmented using a 260-Hounsfield unit (HU) threshold to isolate the bone from the surrounding soft tissue.<sup>14</sup> Manual editing was used to fill in any sections of bone that were not included in the original threshold, or to remove sections of scan metal artifact. The model was then cleaned and smoothed using a gaussian filter to ensure a representative surface (Fig. 1, A). The glenoid implant from each patient's postoperative scans was isolated using a high HU value and subtracted from the scapular model, leaving a 3D model of the

bone (Fig. 1, B). The postoperative images were superimposed over the preoperative scans using global alignment (Fig. 2). Once the images aligned on both the CT scan and the 3D model, the postoperative scapula was hidden, leaving the preoperative scapula and the postoperative glenosphere.

Three reference points were identified and marked on the scapula by 2 fellowship-trained orthopedic surgeons on 2 separate occasions at a 3-week interval. The lateral aspect of the base of the coracoid was identified using a standardized view to obtain points accurately in all cases. A sagittal view of the 3D model with locked coordinates where the anterior and posterior borders of the coracoid appear parallel was used (Fig. 3, A). The most posterior ( $C_A$ ) and most anterior ( $C_B$ ) extents of the lateral border of the base of the coracoid were marked on the points where they meet the scapular body. These points were then checked by re-evaluating their positions on the 3D model. The third point was the glenoid defect ( $G_C$ ), which was the point of the glenoid at the site of its deepest erosion.  $G_C$  helped define the most medial aspect of the pathologic glenohumeral joint line. This was identified on the axial cuts using the 2D images (Fig. 3, B). 3D evaluation of the glenoid depth was found to be misleading as there was no uniformity in the pattern of erosion. The 2D axial sequence was noted to reliably identify the maximal depth of the glenoid erosion. This point ( $G_C$ ) was then projected to the 3D segmentation. The plane of the base of the glenosphere ( $B_p$ ) was created using a line parallel to the medialmost extension of the glenosphere. Three parallel planes to  $B_p$  were then created on the 3 previously marked reference points ( $C_A$ ,  $C_B$ , and  $G_C$ ) (Fig. 4).

Using these 4 planes, the depth of the preoperative pathologic glenohumeral joint line was determined using  $G_C$ . This is the apparent joint line that is measured from the lateral aspect of the

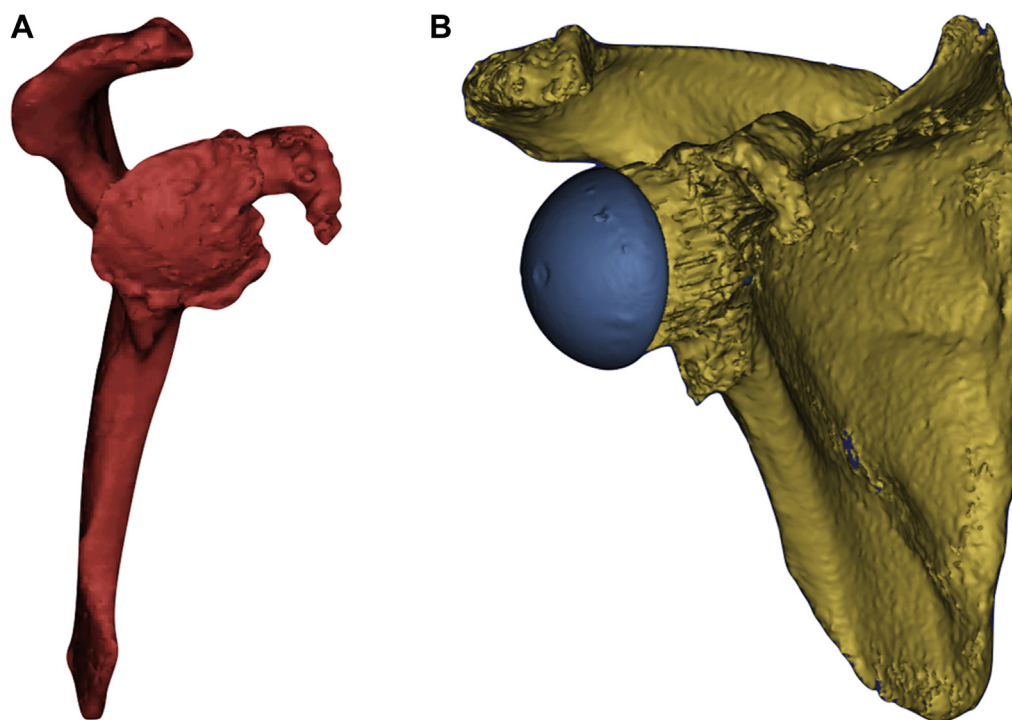


**Figure 1** (A) preoperative 3D scapula model and (B) postoperative 3D model.

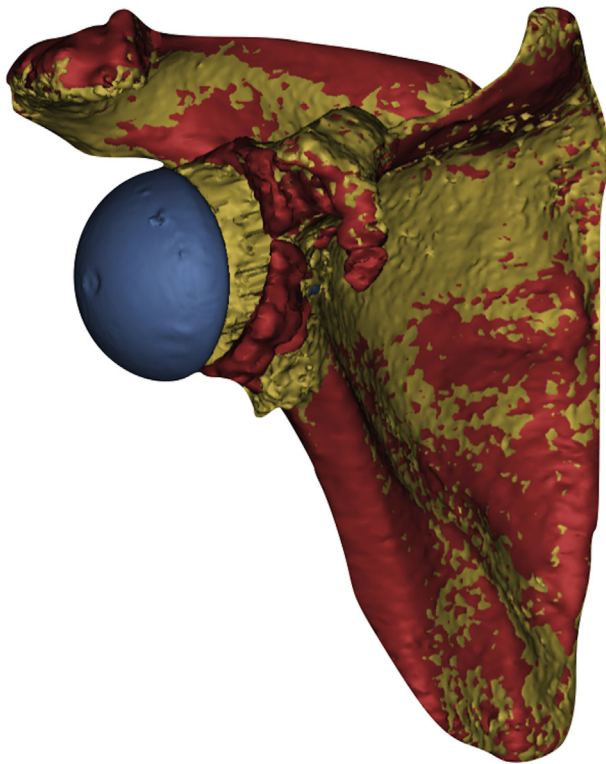


**Figure 2** 3D model of merged preoperative (red) and postoperative (yellow) scans.

base of the coracoid ( $C_A$  and  $C_B$ ) to the most medial point at the base of the glenoid defect ( $G_C$ ) calculated by  $C_A-G_C$  and  $C_B-G_C$ . Postoperative true joint line restoration was measured from the lateral aspect of the base of the coracoid ( $C_A$  and  $C_B$ ) to the base of the glenosphere ( $B_p$ ) calculated by  $C_A-B_p$  and  $C_B-B_p$ . The degree of preoperative medialization and postoperative joint line restoration were assessed based on the normal joint line of 9 mm lateral to base of coracoid.<sup>2,12</sup> Preoperative glenoid defect was calculated by the average of the difference of the normal joint line to  $C_A-G_C$  and  $C_B-G_C$ . Postoperative joint line was calculated by

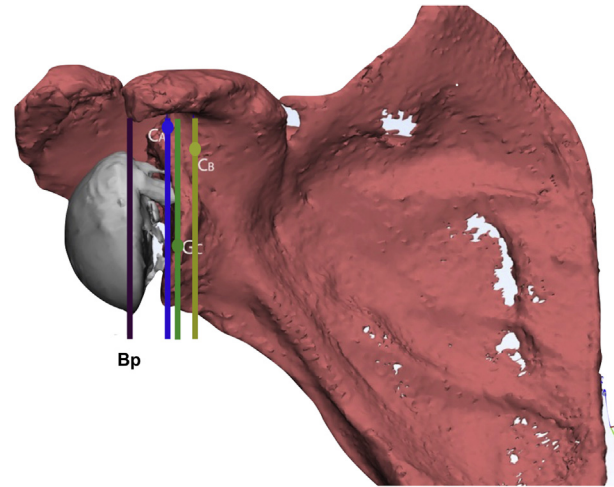


**Figure 4** Coronal view showing reference planes based on  $C_A$ ,  $C_B$ ,  $G_C$ , and  $B_p$ .  $B_p$ , plane of the base of the glenosphere;  $C_A$ , most posterior extent of the lateral aspect of the base of the coracoid;  $G_C$ , deepest erosion on the preoperative glenoid;  $C_B$ , most anterior extent of the lateral aspect of the base of the coracoid.

the average of the difference of the normal joint line to  $C_A-B_p$  and  $C_B-B_p$ . Graft thickness measurements were obtained using the distance from  $G_C$  to  $B_p$ .

Postoperative CT scans were evaluated for graft incorporation, graft resorption, correction of glenoid version, and scapular notching. Graft incorporation was defined as the absence of lucencies at the bone graft–native glenoid interface. The bone graft was deemed to have incorporated into the native glenoid if osseous trabeculae had completely bridged the space between the bone graft and the native glenoid in all the CT coronal and axial slices as defined by Lopiz et al.<sup>25</sup> Graft resorption was defined as bone graft disappearance or grossly visible areas of osteolysis or lucency at the bone-graft interface that was not noted in previous postoperative CT scans. Glenoid version was obtained on the 3D CT reconstructed preoperative and postoperative images of the scapula by measuring the angle formed by the line perpendicular

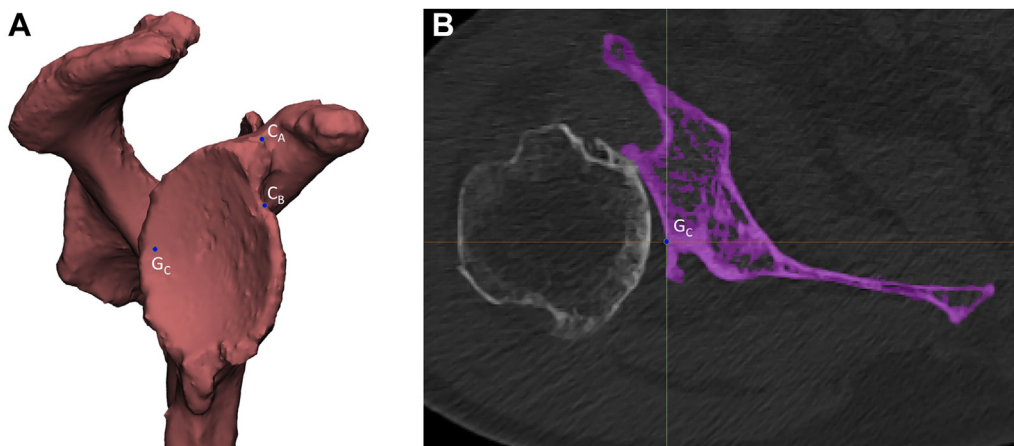


**Figure 3** (A) Sagittal view for marking reference points  $C_A$ ,  $C_B$ , and  $G_C$ . (B)  $G_C$  based on 2D in axial view.  $G_C$ , deepest erosion on the preoperative glenoid;  $C_A$ , most posterior extent of the lateral aspect of the base of the coracoid;  $C_B$ , most anterior extent of the lateral aspect of the base of the coracoid.



to the line from the medial scapular border and glenoid center, and the line from the anterior and posterior glenoid rim at the level of the glenoid center preoperatively and the plane of the baseplate postoperatively.<sup>13</sup> Scapular notching is defined as a defect on the scapular neck inferior to the glenoid component and graded according to the classification by Sirveaux et al.<sup>30</sup>

## Statistical analysis

Mean and standard deviation were calculated for all measurements. The interobserver reliability was evaluated using the intraclass correlation coefficient with points marked by 2 other observers at 2 different occasions using the standardized registration format.

## Operative technique

Humeral head autograft or femoral head allograft is used as structural bone graft to address glenoid bone loss during RSA. Humeral head autografts are used for patients undergoing primary RSA with predominantly central defects on the glenoid. Femoral head allografts are used for revision surgeries and for patients with eccentric defects as these need to be reconstructed using figure-7 graft. The guide pin is inserted into the center of osteotomized humeral head or femoral head allograft. The cannulated glenoid reamer is then inserted through the guide pin, and the surface of the humeral head or femoral head allograft is reamed until the subchondral plate is removed. The central hole is then drilled using the central guide. With the drill left in place, the graft is shaped in a symmetric block for small to moderate centric-eccentric defects, wedge circular block for small to moderate eccentric defects, or a figure-7 configuration for large and massive eccentric defects. This is done manually using saw and handheld high-speed burr ("Craft the graft"). Central peg drill is removed, and graft is positioned at the underside of the glenoid baseplate with a long central peg (Fig. 5). The graft is further sculpted around the implant using a high-speed burr. A minimum graft thickness of 1 cm is ensured. Maximal graft thickness is not measured as complex shapes of the graft often precluded such measurements. In addition, during fixation, the graft undergoes a degree of compression, which results in slight compressive thinning of the graft itself. The glenoid is slightly reamed to flatten the high sides. Areas of the glenoid that are not reamed are curetted and small drill holes using a threaded pin are made to facilitate bleeding. The baseplate with the graft is then impacted onto the native glenoid with a 10° inferior inclination and neutral to slight anteversion. This step is done manually but strictly guided by the direction of the guidewire as planned in the preoperative templating. A minimum of 3 screws are then employed for fixation of the graft through the baseplate and into the glenoid. Anterior-to-posterior screw fixation is added for larger eccentric defects reconstructed using the figure-7 allograft (Fig. 6). In cases of advanced centric-eccentric glenoid defects wherein the long central peg does not purchase a minimum of 50% of its length in the native scapula, bone grafting of the defect is done initially and arthroplasty is performed as a second-stage procedure. A 155° Grammont design (DePuy [Warsaw, IN, USA] DELTA XTEND Reverse Shoulder prosthesis or Wright Medical [Memphis, TN, USA] AEQUALIS Reverse II prosthesis) along with a 42-mm glenosphere is used in all cases.

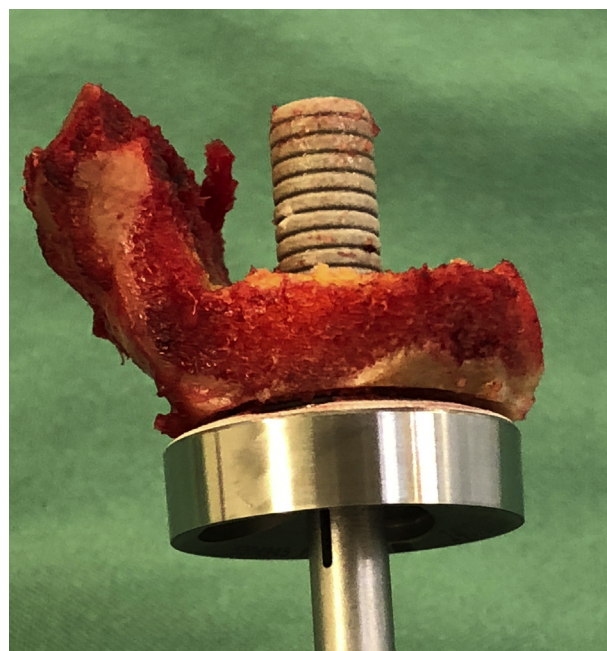


**Figure 5** Figure-7 bone graft.

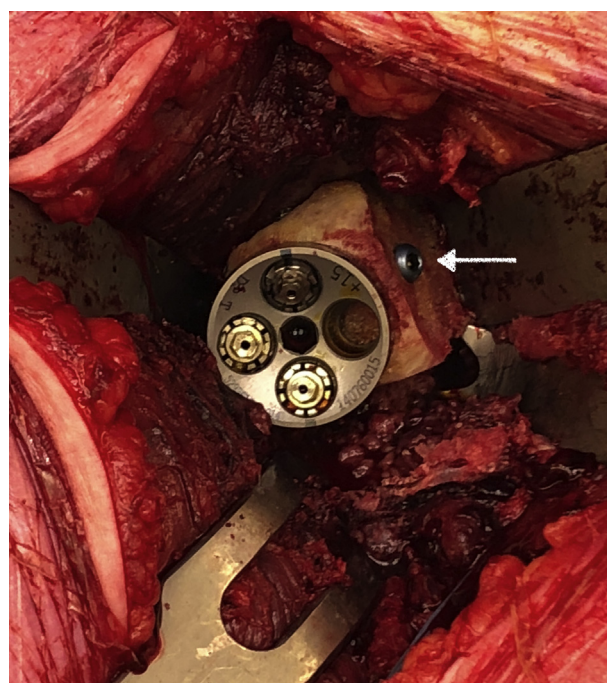


**Figure 6** Intraoperative view of the glenoid with a figure-7 bone graft fixed with compression screw from anterior to posterior (white arrow).

## Postoperative rehabilitation

Patients are immobilized using a shoulder brace with 60° abduction for 6 weeks. They are allowed to be off sling daily during exercises and shower. Patients are encouraged to do active range of motion of the elbow and to use the hand for activities of daily living including eating and drinking. Passive range of motion exercises of the shoulder, such as wall walks, are allowed from

day 1 postoperatively, permitted within pain tolerance. Active range of motion exercises of the shoulder are commenced at 2 weeks postoperatively and strengthening exercises commenced at 8 weeks postoperatively. Return to full activities is generally permitted 3-6 months after surgery.

## Results

A total of 106 patients underwent primary and revision RSA. Out of these, 26 patients underwent RSA with glenoid bone grafting. Five patients were excluded because of follow-up of less than 3 months, 1-stage revision, and self-exclusion from participation. The preoperative glenoid defects were massive (5%), large (29%), moderate (52%), and small (14%). Indications for RSA were osteoarthritis (43%), cuff tear arthropathy (23%), proximal humeral fracture-dislocation (14%), periprosthetic infection (5%), rheumatoid arthritis (5%), irreparable cuff tear (5%), and chronic shoulder dislocation (5%). Twenty cases (95%) were primary RSA; 1 (5%) was 2-stage revision (Table I). All glenoid defects could be satisfactorily reconstructed as a single-stage grafting procedure. Grammont design implants and a baseplate with long peg was used in all the patients (15 [71%] DePuy DELTA XTEND Reverse Shoulder prosthesis, 6 [29%] Wright Medical AEQUALIS Reverse II prosthesis). The mean radiographic follow-up was 19.5 months (range 6-29 months). No patients were lost to follow-up.

The preoperative defects were 2.0 mm medial to C<sub>A</sub> and 3.3 mm lateral to C<sub>B</sub>. The average preoperative defect was noted to be 8.4 mm medial to native joint line or 0.6 mm (range -16.8 to 13.2) lateral to the coracoid base. Postoperatively, the joint line was measured at a mean of 9.0 mm lateral to C<sub>A</sub> and 15.2 mm lateral to C<sub>B</sub>. The postoperative mean joint line was 3.1 mm lateral to the native joint line or 12.1 mm (range 1.3-22.4) lateral to the coracoid base. Mean graft thickness of 12.0 mm (range 5.0-26.5) was measured at final follow-up. Preoperative and postoperative glenoid version measurements are summarized in Table II.

CT scan showed bone graft incorporation in all patients at 3 months postoperatively. No radiolucent lines were observed at the bone graft-native glenoid interface. No scapular notching was observed at final follow-up. Sequential follow-up CT scans showed that 1 patient had grossly evident graft resorption at 1 year. This patient presented with persistent pain on the shoulder and limited range of motion. The patient subsequently underwent 2-stage revision surgery. All biopsies sent for culture had no growth of any microorganisms. Graft resorption in this case was attributed to the patient's medical comorbidities, including cryoglobulinemia on regular plasmapheresis and chronic lung disease managed on long-term steroids. Glenoid grafting was performed during the index surgery as a result of intraoperative glenoid rim fracture and

**Table I** Patient demographic characteristics

Variable	
Number of patients, n	21
Mean age, yr (standard deviation)	71.05 (7.49)
Sex, n (%)	
Male	11 (52)
Female	10 (48)
Operative side, n (%)	
Right	14 (67)
Left	7 (33)
Indication for surgery, n (%)	
Osteoarthritis	9 (43)
Cuff tear arthropathy	5 (23)
Proximal humerus fracture-dislocation	3 (14)
Periprosthetic infection	1 (5)
Rheumatoid arthritis	1 (5)
Irreparable cuff tear	1 (5)
Chronic dislocation	1 (5)
Stage, n (%)	
Primary	20 (95)
2-stage revision	1 (5)
Preoperative defects, n (%) <sup>*</sup>	
Small	3 (14)
Medium	11 (52)
Large	6 (29)
Massive	1 (5)
Bone graft type, n (%)	
Humeral head autograft	15 (71)
Femoral head allograft	6 (29)
Implants	
DePuy DELTA XTEND Reverse Shoulder prosthesis	15 (71)
Wright Medical AEQUALIS Reverse II prosthesis	6 (29)

<sup>\*</sup> Based on the Gupta-Seebauer classification. Small = C1/E1; medium = C2/E1, C1/E2, C2/E2; large = C1/E3, C2/E3, C3/E1, C3/E3; massive = C3/E4.

unavailability of metallic augments. An augmented baseplate was used during revision surgery instead of an allograft to re-create the native joint line. At the latest follow-up, the patient continued to improve in pain and functional terms.

The interobserver reliabilities and their 95% confidence intervals were based on a single-rating, consistency agreement and 2-way mixed effects model. The average measured intraclass correlation coefficient for the measurements were 0.987 (0.980-0.992) which represented an excellent degree of interrater reliability.<sup>24</sup>

## Discussion

Glenoid bone erosion is frequently encountered in patients undergoing shoulder arthroplasty. This abnormal glenoid morphology is shown to be present in 37.5%-39% of patients undergoing primary RSA.<sup>13,23</sup> In our series, 25% of

**Table II** Preoperative and postoperative radiographic outcomes

Variable	Mean (SD), range; or n/n (%)
Preoperative glenoid defect (apparent glenoid joint line)*, mm	
C <sub>A</sub> to G <sub>C</sub>	-2.0 (5.2), -16.8 to 5.5
C <sub>B</sub> to G <sub>C</sub>	3.3 (6.7), -9.3 to 13.2
Postoperative restoration (true glenoid joint line), mm	
C <sub>A</sub> to B <sub>p</sub>	9.0 (3.1), 1.3-15.8
C <sub>B</sub> to B <sub>p</sub>	15.2 (3.8), 9.9-22.4
Graft thickness†, mm	12.0 (5.1), 5.0-26.5
Graft incorporation‡	21/21 (100)
Graft resorption§	1/21 (4.76)
Notching§	0/21 (0)
Version	
Preoperative	-8° (15°), -39° to 22°
Postoperative	-5° (11°), -19° to 24°

C<sub>A</sub>, most posterior extent of the lateral aspect of the base of the coracoid; G<sub>C</sub>, deepest erosion on the preoperative glenoid; C<sub>B</sub>, most anterior extent of the lateral aspect of the base of the coracoid; B<sub>p</sub>, plane of the base of the glenosphere; SD, standard deviation; CT, computed tomographic.

\* A negative value indicates a preoperative defect medial to the lateral aspect of the base of the coracoid.

† This is also equivalent to the net restoration, which is the distance from the preoperative glenoid defect to the baseplate (G<sub>C</sub> to B<sub>p</sub>).

‡ Noted on 3-month postoperative CT scans.

§ Noted on CT scan at mean follow-up of 19.5 months (range 6-29 months).

|| A negative value indicates retroversion.

patients had significant acquired glenoid bone loss, most of which were medium to large bone defects.

The presence of significant glenoid bone erosion has been shown to have undesirable effects on the outcomes after shoulder arthroplasty.<sup>18</sup> Frankle et al<sup>13</sup> reported that most glenoid erosions are located posteriorly, causing excessive retroversion. This results in implant malpositioning if not appropriately addressed. Shapiro et al demonstrated in cadaveric specimens that placement of glenoid component in 15° of retroversion significantly decreased the glenohumeral contact area, increased contact pressures, and decreased inferior and posterior glenohumeral forces.<sup>29</sup> This increases the risk of implant loosening and affects the intrinsic stability of the construct.<sup>9,10,27</sup>

Presence of significant glenoid bone loss also compromises the bone stock. Having poor bone stock affects the initial strength and stability of fixation. Through a biomechanical study, Codsí et al<sup>7</sup> proved that the presence of large central cavitory defect, usually seen in revision settings, resulted in greater micromotion of the glenoid

implant, especially if fixed with standard screw fixation. This greatly affected the initial fixation and stability of the construct.<sup>7</sup>

Different surgical techniques have been described in literature for glenoid bone grafting to address cases of significant bone defects. Boileau et al<sup>3,4</sup> introduced the concept of BIO-RSA wherein a disc of bone graft is harvested from the native humeral head and placed in between the reamed glenoid and the baseplate. The studies did not specifically evaluate restoration of glenoid joint line but focused on correction of glenoid version and inclination. They reported that the bone graft restores glenoid bone stock and allows correct baseplate alignment. They have established that using bone graft allows lateralization of the baseplate and sphere, which provides good functional results, comparable to those of RSA without glenoid deficiency. They also reported that this avoids instability and severe scapular notching.

In 2012, Bateman and Donald<sup>1</sup> described a bone grafting technique using a combination of autograft and allograft to reconstruct massive uncontained glenoid defects. They used the femoral neck allograft as a peripheral cortical ring compressed onto the native glenoid. The central defect was then impacted with cancellous autograft from the native humeral head, iliac crest, or the Gerdy tubercle. With this technique, they aimed to restore the bony surface of the glenoid at least to the level of the base of the coracoid.

Despite this increasing interest in glenoid bone grafting, the appropriate amount of joint line restoration is still undetermined. Previous studies have focused on restoration of the glenoid deformity, graft incorporation, scapula notching, correction of version and inclination on bone grafting, and RSA.<sup>3,4,22,25,26,32</sup> Our series has confirmed that structural bone grafting of the glenoid effectively recreates the glenoid anatomy, restores glenoid bone stock, and re-creates the true glenohumeral joint line. We found that a mean bone graft thickness of 12 mm (range 5.0-26.5 mm) was able to restore the normal joint line of a preoperatively medialized glenoid and improve glenoid version. Based on the reference normal glenohumeral joint line of 9 mm lateral to the base of the coracoid, there is a small amount of glenoid-sided lateralization attained from our technique of bone grafting.<sup>2,12</sup> This could potentially contribute to better impingement-free range of motion and less risk of scapular notching, particularly in our technique that uses Grammont design prosthesis.<sup>2,9,25,27</sup> Despite the use of Grammont design prostheses in our patients, we did not note any scapular notching at final follow-up. Inferior scapular notching due to impingement of the humeral insert against the scapula secondary to the medialized design of the Grammont prosthesis has reported rates as high as 96% in postoperative radiographs.<sup>3</sup> The absence of scapular notching in our series may be attributed to the amount of lateralization achieved by the bone grafting, along with the inferior tilt of 10°, inferior placement of the glenosphere,



and the use of larger glenosphere (42 mm).<sup>3</sup> Our series shows that with a medialized Grammont prosthesis, the risk of scapular impingement and notching is decreased when the glenoid joint line is restored and proper implant placement is achieved in patients with significant glenoid erosion. Scapular notches can become evident on radiographs at 6 months after surgery.<sup>3</sup> Our patients were routinely followed up using CT scans, and no notching was observed at mean follow-up of 19.5 months (range 6–29). Despite this, longer observation may be necessary to monitor the development of notching in our technique.

Our measurements were referenced from the base of the coracoid as this is a constant anatomic landmark of the shoulder. The base of the coracoid is a structure that is least likely to be involved in glenoid erosions. This is a palpable anatomic structure that can be easily visualized intraoperatively. There is currently no standardized guidance method to establish the base of the coracoid. We chose 2 reference points on the lateral aspect of the base of the coracoid marked on standardized views to ensure consistent and reproducible measurements. Literature reports several different ways of evaluating glenoid erosion and depth of erosion, and measuring the glenoid joint line.<sup>2,12,13,17,31</sup> Most of these were measured on 2D images. Plain radiographic analysis has a limitation of projectional error caused by the positioning of the scapula on the thorax. In our study, we have used standardized medical computer-aided design (CAD) software to create 3D reconstructed images from CT scans. Advanced image segmentation techniques were employed in our study aiming to address some of the limitations faced in the past. In addition, evaluation of the glenoid joint line is often established from the rim of the residual glenoid and not the deepest, most medial point. Although topographical cadaveric studies are akin to using the enface 3D CT view to evaluate the depth of glenoid erosion, we found this method highly unreliable to delineate the deepest, most medial point of the erosion. Axial 2-D CT scan images need to be employed to evaluate this.

Our study also showed high percentage of graft healing, which was consistent with the previous literature showing good graft incorporation after bone grafting and RSA.<sup>3,4,22,25</sup> In our series, at 3 months' follow-up, all patients had graft healing, which is higher than the healing rates in other published literature.<sup>3,4,22,25</sup> This can be attributed to the compressive forces brought about by the RSA construct. The postoperative immobilization at 60° abduction negates shear forces on the baseplate-graft construct. This helps maintain the compressive force, thereby further increasing the possibility of bone graft incorporation into the native glenoid. Drill holes are made on the sclerotic areas on the glenoid that is not reamed to allow bleeding, which could potentially facilitate healing of the bone graft onto the native glenoid.

Our results demonstrate that glenoid bone grafting using autograft humeral head or allograft femoral head shaped into a tailored cortico-cancellous disc, a wedge, or figure-7

graft is a reliable method to restore the glenoid joint line and correct glenoid deformity with good graft incorporation. Grafting has 3 main advantages. It provides a biological solution and helps build bone in a deficient glenoid ensuring restoration of bone stock, which is helpful in the case of future revision. Tailored grafts can be custom-made intraoperatively for adequate shapes, sizes, and thickness depending on glenoid defects. Humeral autograft provides a cheap and readily available option in situations where a surgeon may not have access to augmented implants.

One of the limitations of our study was the inability to evaluate resorption of the graft at the baseplate–bone graft interface. This is due to the current CT scatter segmentation difficulty brought about by metal artifacts. This has previously been reported by Ferreira et al<sup>11</sup> in their study on the effectiveness of CT for the detection of glenoid bone graft resorption. Using cadaveric specimens, they found that CT has low sensitivity and accuracy in detecting the presence or absence of bone graft resorption adjacent to glenoid baseplate (38% and 46%, respectively). Even experienced observers were not able to consistently identify defects up to 8 mm between the bone graft and the glenoid baseplate. We were, however, able to identify 1 patient with graft resorption, which was grossly evident on the 1-year CT scan follow-up. This patient was also clinically symptomatic, presenting with persistent shoulder pain and limited range of motion. This complication was attributed to the patient's medical comorbidities particularly affecting bone healing capacity. With this, it is advised that careful patient selection should be observed when addressing significant glenoid bone defects during RSA. We hypothesized that alternative techniques to restore glenoid joint line should be considered in patients with medical comorbidities known to affect bone healing.

Another limitation of this study is that the measurements performed relied on manually placed points on 3D images. Although this may be more accurate than using 2D images, manually placed points may have affected the accuracy of the measurements. Despite this, we were able to achieve excellent interobserver reliability by establishing standardized techniques for manual placement of reference points.<sup>24</sup>

## Conclusion

Significant glenoid erosion during RSA poses undesirable outcomes if not recognized and addressed appropriately. The use of structural bone grafting during RSA has been shown to effectively restore the true joint line in patients with medialized apparent joint line due to significant glenoid bone loss. An average bone graft thickness of 12 mm can restore a preoperative joint line of 0.6 mm lateral to the base of the coracoid. It improves glenoid version and provides quantifiable lateralization,



which could potentially contribute to less risk of notching especially when a Grammont design prosthesis is used. It is a safe and reproducible technique, with a high graft incorporation rate at 3 months postoperatively. Careful patient selection should be observed, as patients with medical comorbidities affecting bone healing may not be good candidates for glenoid bone grafting. Further research is needed to improve segmentation techniques to reliably evaluate graft lysis at the baseplate-graft interface and to automate point placement in order to obtain more accurate measurements.

## Disclaimer

The authors, their immediate families, and any research foundations with which they are affiliated have not received any financial payments or other benefits from any commercial entity related to the subject of this article.

## References

- Bateman E, Donald SM. Reconstruction of massive uncontained glenoid defects using a combined autograft-allograft construct with reverse shoulder arthroplasty: preliminary results. *J Shoulder Elbow Surg* 2012;21:925-34. <https://doi.org/10.1016/j.jse.2011.07.009>
- Bhatia DN, de Beer JF, du Toit DF. Coracoid process anatomy: implications in radiographic imaging and surgery. *Clin Anat* 2007;20:774-84. <https://doi.org/10.1002/ca.20525>
- Boileau P, Moineau G, Roussanne Y, O'Shea K. Bony increased-offset reversed shoulder arthroplasty: minimizing scapular impingement while maximizing glenoid fixation. *Clin Orthop Relat Res* 2011;469:2558-67. <https://doi.org/10.1007/s11999-011-1775-4>
- Boileau P, Morin-Salvo N, Gauci MO, Seeto BL, Chalmers PN, Holzer N, et al. Angled BIO-RSA (bony-increased offset-reverse shoulder arthroplasty): a solution for the management of glenoid bone loss and erosion. *J Shoulder Elbow Surg* 2017;26:2133-42. <https://doi.org/10.1016/j.jse.2017.05.024>
- Chen X, Reddy AS, Kontaxis A, Choi DS, Wright T, Dines DM, et al. Version correction via eccentric reaming compromises remaining bone quality in B2 glenoids: a computational study. *Clin Orthop Relat Res* 2017;475:3090-9. <https://doi.org/10.1007/s11999-017-5510-7>
- Clavert P, Millett PJ, Warner JJP. Glenoid resurfacing: what are the limits to asymmetric reaming for posterior erosion? *J Shoulder Elbow Surg* 2007;16:843-8. <https://doi.org/10.1016/j.jse.2007.03.015>
- Codsi MJ, Iannotti JP. The effect of screw position on the initial fixation of a reverse total shoulder prosthesis in a glenoid with a cavitory bone defect. *J Shoulder Elbow Surg* 2008;17:479-86. <https://doi.org/10.1016/j.jse.2007.09.002>
- Endrizzi DP, Mackenzie JA, Henry PDG. Early debris formation with a porous tantalum glenoid component: radiographic analysis with 2-year minimum follow-up. *J Bone Joint Surg Am* 2016;98:1023-9. <https://doi.org/10.2106/JBJS.15.00410>
- Farron A, Terrier A, Büchler P. Risks of loosening of a prosthetic glenoid implanted in retroversion. *J Shoulder Elbow Surg* 2006;15:521-6. <https://doi.org/10.1016/j.jse.2005.10.003>
- Favre P, Sussmann PS, Gerber C. The effect of component positioning on intrinsic stability of the reverse shoulder arthroplasty. *J Shoulder Elbow Surg* 2010;19:550-6. <https://doi.org/10.1016/j.jse.2009.11.044>
- Ferreira LM, Knowles NK, Richmond DN, Athwal GS. Effectiveness of CT for the detection of glenoid bone graft resorption following reverse shoulder arthroplasty. *Orthop Traumatol Surg Res* 2015;101:427-30. <https://doi.org/10.1016/j.otsr.2015.03.010>
- Fortun CM, Gobeze R, Streit JJ, Horton SA, Muh SJ, Gillespie RJ. Scapular neck length and implications for reverse total shoulder arthroplasty: an anatomic study of 442 cadaveric specimens. *Int J Shoulder Surg* 2015;9:38-42. <https://doi.org/10.4103/0973-6042.154754>
- Frankle MA, Teramoto A, Luo ZP, Levy JC, Pupello D. Glenoid morphology in reverse shoulder arthroplasty: classification and surgical implications. *J Shoulder Elbow Surg* 2009;18:874-85. <https://doi.org/10.1016/j.jse.2009.02.013>
- Green N, Glatt V, Tetsworth K, Wilson LJ, Grant CA. A practical guide to image processing in the creation of 3D models for orthopedics. *Tech Orthop* 2016;31:153-63. <https://doi.org/10.1097/BTO.0000000000000181>
- Gupta A, Thussbas C, Koch M, Seebauer L. Management of glenoid bone defects with reverse shoulder arthroplasty—surgical technique and clinical outcomes. *J Shoulder Elbow Surg* 2018;27:853-62. <https://doi.org/10.1016/j.jse.2017.10.004>
- Habermeyer P, Magosch P, Lichtenberg S. Recentering the humeral head for glenoid deficiency in total shoulder arthroplasty. *Clin Orthop Relat Res* 2006;457:124-32. <https://doi.org/10.1097/BLO.0b013e31802ff03c>
- Iannotti JP, Gabriel JP, Schneck SL, Evans BG, Misra S. The normal glenohumeral relationships: an anatomical study of one hundred and forty shoulders. *J Bone Joint Surg Am* 1992;74:491-500.
- Iannotti JP, Norris TR. Influence of preoperative factors on outcome of shoulder arthroplasty for glenohumeral osteoarthritis. *J Bone Joint Surg Am* 2003;85:251-8. <https://doi.org/10.2106/00004623-200302000-00011>
- Ivaldo N, Mangano T, Caione G, Rossoni M, Ligas A. Customized tantalum-augmented reverse shoulder arthroplasty for glenoid bone defect and excessive medialization: description of the technique. *Musculoskelet Surg* 2016;100(Suppl 1):S13-8. <https://doi.org/10.1007/s12306-016-0404-5>
- Jones RB. Addressing glenoid erosion in anatomic total shoulder arthroplasty. *Bull Hosp Jt Dis* 2013;71(Suppl 2):S46-50. PMID: 24328580.
- Jones RB, Wright TW, Roche CP. Bone grafting the glenoid versus use of augmented glenoid baseplates with reverse shoulder arthroplasty. *Bull Hosp Jt Dis* 2015;73(Suppl 1):S129-35.
- Kirzner N, Paul E, Moaveni A. Reverse shoulder arthroplasty vs BIO-RSA: clinical and radiographic outcomes at short term follow-up. *J Orthop Surg Res* 2018;13:256. <https://doi.org/10.1186/s13018-018-0955-2>
- Klein SM, Dunning P, Mulieri P, Pupello D, Downes K, Frankle MA. Effects of acquired glenoid bone defects on surgical technique and clinical outcomes in reverse shoulder arthroplasty. *J Bone Joint Surg Am* 2010;92:1144-54. <https://doi.org/10.2106/JBJS.1.00778>
- Koo TK, Li MY. A guideline of selecting and reporting intraclass correlation coefficients for reliability research. *J Chiropr Med* 2016;15:155-63. <https://doi.org/10.1016/j.jcm.2016.02.012>
- Lopez Y, García-Fernández C, Arriaza A, Rizo B, Marcelo H, Marco F. Midterm outcomes of bone grafting in glenoid defects treated with reverse shoulder arthroplasty. *J Shoulder Elbow Surg* 2017;26:1581-8. <https://doi.org/10.1016/j.jse.2017.01.017>
- Mahylyis JM, Puzzitiello RN, Ho JC, Amini MH, Iannotti JP, Ricchetti ET. Comparison of radiographic and clinical outcomes of revision reverse total shoulder arthroplasty with structural versus nonstructural bone graft. *J Shoulder Elbow Surg* 2019;28:e1-9. <https://doi.org/10.1016/j.jse.2018.06.026>
- Seidl AJ, Williams GR, Boileau P. Challenges in reverse shoulder arthroplasty: addressing glenoid bone loss. *Orthopedics* 2016;39:14-23. <https://doi.org/10.3928/01477447-20160111-01>

28. Service BC, Hsu JE, Somerson JS, Russ SM, Matsen FA 3rd. Does postoperative glenoid retroversion affect the 2-year clinical and radiographic outcomes for total shoulder arthroplasty? *Clin Orthop Relat Res* 2017;475:2726-39. <https://doi.org/10.1007/s11999-017-5433-3>
29. Shapiro TA, McGarry MH, Gupta R, Lee YS, Lee TQ. Biomechanical effects of glenoid retroversion in total shoulder arthroplasty. *J Shoulder Elbow Surg* 2007;16:90S-5S. <https://doi.org/10.1016/j.jse.2006.07.010>
30. Sirveaux F, Favard L, Oudet D, Huquet D, Walch G, Mole D. Grammont inverted total shoulder arthroplasty in the treatment of glenohumeral osteoarthritis with massive rupture of the cuff. *J Bone Joint Surg Br* 2004;86:388-95. <https://doi.org/10.1302/0301-620X.86B3.14024>
31. Takase K, Yamamoto K, Imakiire A, Burkhead WZ. The radiographic study in the relationship of the glenohumeral joint. *J Orthop Res* 2004;22:298-305. [https://doi.org/10.1016/S0736-0266\(03\)00187-6](https://doi.org/10.1016/S0736-0266(03)00187-6)
32. Tashjian RZ, Granger E, Chalmers PN. Structural glenoid grafting during primary reverse total shoulder arthroplasty using humeral head autograft. *J Shoulder Elbow Surg* 2018;27:e1-8. <https://doi.org/10.1016/j.jse.2017.07.010>
33. Wang T, Abrams GD, Behn AW, Lindsey D, Giori N, Cheung EV. Posterior glenoid wear in total shoulder arthroplasty: eccentric anterior reaming is superior to posterior augment. *Clin Orthop Relat Res* 2015;473:3928-36. <https://doi.org/10.1007/s11999-015-4482-8>